

DockSurf: A molecular modeling software for the prediction of protein/surface adhesion.

Authors:

F. Barbault^{1*}, E. Brémond¹, J. Rey², P. Tufféry² and F. Maurel¹

Address:

*corresponding author

1: Université Paris Cité, CNRS, ITODYS, F-75013 Paris, France.

2: Université Paris Cité, CNRS UMR 8251, INSERM U1133, RPBS, Paris, France.

Keywords: biomaterials, docking, protein surface interface, software

Abstract:

The elucidation of structural interfaces between proteins and inorganic surfaces is a crucial aspect of bionanotechnology development. Despite its significance, the interfacial structures between proteins and metallic surfaces have yet to be fully understood, and the lack of experimental investigation has impeded the development of many devices. To overcome this limitation, we suggest considering the generation of protein/surface structure as a molecular docking problem with a homogenous plan as the target. To this extent we propose a new software, DockSurf which aims to quickly propose reliable protein/surface structure. Our approach considers the conformational exploration with Euler's angles, which provide a cartography instead of a unique structure. Interaction energies were derived from QM computations for a set of small molecules that describe protein atom-types, and implemented in a DLVO potential for the consideration of large systems such as proteins. The validation of DockSurf software was conducted with molecular dynamics for corona proteins with gold surfaces and provided enthusiastic results. This software is implemented in the RPBS platform to facilitate widespread access to the scientific community.

Introduction:

One key aspect in the development of bionanotechnologies is the elucidation of the structural interfaces between proteins and inorganic surfaces¹. Many biological and therapeutic examples illustrate these associations like hard tissue growth such as bones or dentine², medical implants³, drug-delivery⁴ and nanotoxicity⁵. Besides, nanodevices such as biosensors⁶, biologically inspired antifouling polymers^{7,8} and molecular imprinted polymers^{9,10} generally involve protein/surface interaction. Describing and understanding the nature of molecular recognition between an inorganic surface and a protein is paving the way towards rationalization, optimization and prediction of many biotechnology devices¹¹.

Despite its wide importance, the experimental investigations of proteins adsorbed onto inorganic surfaces still remain elusive¹². In this context, molecular simulations represent an affordable alternative to understand the underlying physical processes which occur at the protein/surface interface¹. In this context, according to the size of proteins and water environment, molecular

mechanics (MM) strategy is certainly the more practical way to decipher their interaction with inorganic surfaces even if this requires specific force-field parameterizations. During the last decade, several works have been devoted to this goal for various types of inorganic surfaces¹³⁻¹⁹ and molecular dynamics (MD) appears to be most reliable technique to perform the required conformational explorations to study the protein adsorption onto solid surfaces^{1,12,20}.

Notwithstanding its effectiveness, a MD simulation still heavily relies on the protein's initial orientation and position upon the inorganic surface²¹. To overcome this drawback, a common remedy consists in starting several MD simulations with various initial orientation/position. Since this strategy drastically increases the computational time, several practical assumptions have been made which either considers the protein as a rigid body in implicit solvent²² or flexible, but in vacuo²³. One other alternative is to rotate the protein like a dice and to conduct 6 MD simulations²⁴ for, at least, 100 ns under water periodic conditions. In all cases, the achievements of these structural investigations require the access to high performance computational facilities and a strong expertise in the topic.

In order to expedite the initialization of molecular dynamics (MD) computations, our study proposes an innovative docking approach that seeks to identify the most stable association between a protein and a surface. Molecular docking is a widely used computational technique in drug-design strategies that efficiently and quickly determines the optimal orientation of a small organic ligand inside a biomolecule cavity to inhibit its activity²⁵. Our team has a strong expertise on molecular docking technique applied and/or developed for RNA/ligand^{26,27}, DNA/ligand²⁸, protein/ligand²⁹ and even protein/protein³⁰ complexes. In this study, we extend this approach to include protein/surface systems, both organic and inorganic, and integrate it into the DockSurf software package, a user-friendly and free web interface that is directly linked to the PDB database. Consequently, any user, regardless of their familiarity with molecular modeling, can use the software to predict the interaction of their protein coordinates or even a pdb code.

Overview and computational details

a) Energy computations and fitting:

The potential energies were then recorded at the quantum mechanics (QM) level with DFT (PBE0-D3(BJ) LanLD2Z+gold pseudopotential and 6-31+G* with Gaussian16 software³¹ and at the molecular mechanics (MM) level with the interface¹⁵ and gaff2³² force fields implemented in Amber20 software³³. To do this, small molecules mimicking the molecular diversity of proteins (see later) are slowly approached to a Au{111} surface.

b) Molecular dynamics:

Molecular dynamics simulations (MD) were conducted to validate the docking poses of proteins onto the gold surface with the Amber 20³³ software within the interface¹³ force-field for Au{111} and ff14SB³⁴ for proteins. Each considered systems were embedded in a water periodic box with TIP3P³⁵ and minimized with weak harmonic restraints (0.5 kcal/mol) on solute (surface + protein). A second minimization for the whole system without restraint is performed before the heating phase where the system temperature slowly rises from 0 to 300 K. After a solvent equilibration in the NTP ensemble for 1 ns, a production is performed in the NVT ensemble for trajectories between 50 ns to 200 ns, according to the explorations considered. Visualizations and analyses of MD trajectories were

made with VMD³⁶ and cpptraj³⁷ software, respectively.

When applicable, free energy of protein/surface adsorption were obtained through a MMGBSA strategy³⁸. The following equations were employed:

$$\begin{aligned} \text{Protein} + \text{Gold} &\rightarrow \text{complex} \\ \langle \Delta G_{\text{binding}} \rangle &= \langle G_{\text{complex}} \rangle - (\langle G_{\text{Protein}} \rangle + \langle G_{\text{Gold}} \rangle) \\ \langle G_i \rangle &= \langle E_i^{\text{gas}} \rangle + \langle G_i^{\text{solvent}} \rangle \\ \langle G_i^{\text{solvent}} \rangle &= \langle G_i^{\text{polar}} \rangle + \langle G_i^{\text{non-polar}} \rangle \end{aligned}$$

This calculation was employed for the last 20 ns of 50 ns MD trajectories ensuring this way that equilibrations are reached for all systems. Each 5 ps were considered, so that the averages (values in brackets) of the equations above were made for 4 000 conformations. Subscripts i represent the species used for the calculation (complex, protein or gold surface alone). According to the rigid nature of gold surface, gas-phase entropies variations were not computed.

c) General overview

DockSurf software runs as a batch job with predetermined inputs to process computations and analyze output data, it can be launched with a single command line, enabling this way automated computation of protein database structures and the implementation on free web server as exemplified on this article. Typical run looks like:

```
> DockSurf label pdbfile fine surfacetype sel
clusconf
```

In the above input, 'label' is a nickname which will be used to name and identify all output files and 'pdbfile' is the filename of the protein 3D coordinates. This last file must be exclusively in the protein databank format³⁹, which is - by far - the most used file format. The 'fine' parameter specifies the angle step to rotate the protein through Euler's angles (typical values 5 or 10°) and 'surfacetype' is a tag for the surface type. To date, only gold Au{111} has been parametrized but the software is designed to be easily upgraded for other surface types. The 'sel' tag is a integer which determines the number of desired output protein/surface structures. 'clusconf' is a string which can be either 'conf' or 'clus' and defines if a 10° clustering is made (clus) or if the selection is solely made with energy ranking (conf). Figure 1 illustrates the code flow and highlights the inputs and outputs data.

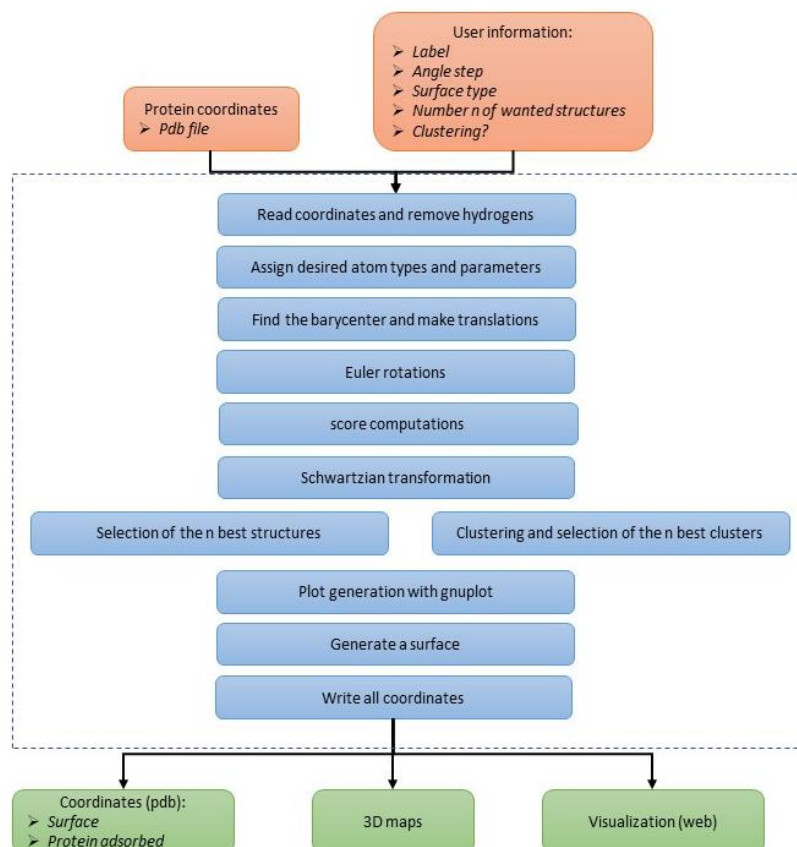


Figure 1: DockSurf program flow. Orange and green colors represent, respectively, the input and output data whereas modules in blue stand for the various phases of the program.

DockSurf utilizes the free software Gnuplot⁴⁰ to generate 3D contour plot images in png format. Gnuplot is typically already available on Linux operating systems and can be easily installed on Windows. All intermediate data, such as Gnuplot scripts or 3D energy data, are preserved and can be further processed with other software as desired by the user.

d) Web server implementation:

A web server access to DockSurf is provided via the RPBS platform⁴¹, using the Moby framework⁴² and it is accessible at "<https://bioserv.rpbs.univ-paris-diderot.fr/services/DockSurf/>". Inputs consist of the coordinates structure of the protein to position over the surface (PDB format), the angular increment to sample the relative orientation of the protein on the surface. Other parameters define the number of selected model to return, and the way they are identified – cluster centroids or individual models. The clustering is defined to 10° as it corresponds to better results

Methods:

The main statement of this study was to tackle the problem of finding the optimal interaction of a

protein on an inorganic surface as a molecular docking question. With this assumption in mind, the optimal interaction of a protein on an inorganic surface can be translated by the finding of the best plane on a protein molecular surface. The best plane is here the plane with the lowest interaction energy.

Like any other molecular docking software, DockSurf, can be regarded as a software able to rapidly explore the phase space and compute the interaction energy²⁵. Thus, the exploration method will be presented prior to the description of the scoring energies while, during the execution of DockSurf, these steps are made at the same phase to speed-up the docking process.

e) Exploration method:

Molecular docking has been widely used for predicting ligand/protein interactions in the context of drug-design (see²⁹ as example) and usually consider solely the flexibility of ligand whereas the protein stays rigid. According to the fact that mineral surfaces are undoubtedly non-flexible, the first hypothesis which can be drawn will consider the protein/surface interaction as a rigid body problem. This assumption is widely used in protein/protein molecular docking software⁴³.

The main goal of the exploration process is to be exhaustive and efficient. Since proteins are considered to be rigid, the process of exploring their structures can be likened to an airplane flying above the ground. This analogy leads to the identification of the degrees of freedom, which is dependent on the definitions of movement. During flight, an airplane moves through three translations along the x, y, and z axis (T_x , T_y , and T_z) with the center of the coordinate system located at the aircraft's center. Rotations are defined around the axis and are known as "roll," "pitch," and "yaw" angles. These angles are used to describe the movement of objects such as proteins and are defined through Euler angles referred to as "precession," "nutation," and "intrinsic rotation," which respectively represent rotation around the principal axes x, y, and z.

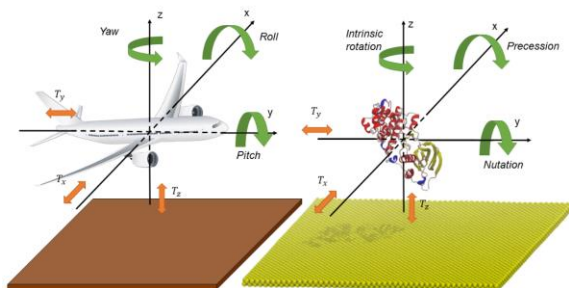


Figure 2: Like an airplane, a protein above a surface has 6 degrees of freedom: 3 translations (T_x , T_y and T_z) and 3 rotations. These last are defined by Euler angles (precession, nutation and intrinsic rotation).

In the context of protein/surface interactions, it is possible to eliminate certain degrees of freedom that describe the movement of a rigid-body, such as a protein. By considering the mineral surface to be flat and uniform, the T_x and T_y translations, along with intrinsic rotation, can be eliminated. Thus, only the T_z translation and precession and nutation rotations are needed to describe the structural organization above the mineral surface. The scoring function can be astutely defined (see later) to consider only two rotations, precession and nutation, in exploring protein movements above the surface and avoiding T_z exploration. Working with only two degrees of freedom allows for an exhaustive exploration of these coordinates, providing a cartography of the protein/surface interaction. Additionally, when exploring the precession angle between 0 and 360°, the nutation angle only needs to be investigated between 0 and 180°. Therefore, an angle step of 10° requires computing 648 structures, while an angle

step of 5° requires computing 2592 structures. The choice of angle step size must be made judiciously, as a small value (<4°) leads to long computation times, while a large value (>20°) drastically reduces calculation accuracy.

f) Scoring energies:

In molecular docking, it is crucial to efficiently evaluate interaction energy to explore the space of orientations extensively. For example, popular protein/ligand molecular docking software like Autodock⁴⁴ or Vina⁴⁵ compute crudely the association energy as a combination points on grids. As a result, in protein/surface docking software, the energy computation only needs to provide a qualitative ranking of the conformations rather than an accurate assessment of the association energy. This allows for a faster exploration of the docking space. Given this context, a novel approach was pursued to compute energy through a customized force field :

- Select small molecules that adequately represent the chemical diversity of protein amino-acids.
- Determine the energy interaction as a function of the normal distance to the gold surface, using quantum and molecular mechanics methods.
- Fit this energy curve to a potential with an equation containing only few parameters.
- Divide this contribution to an atomic contribution considering only the heavy atoms of fragments.

The association energy calculation for huge molecular object such as protein requires a force-field approximation. To this extent, nine small molecules, depicted in Figure 3, were selected. These include acetamide, which is used to parametrize the peptide backbone and tail parts of Gln and Asn amide moieties. Aromatic residues such as Phe, Tyr, and Trp were represented using benzene, while imidazole was employed for His and Trp. Methane was used to parametrize all alkyl sp^3 carbons found in residue side chains. Ionic molecules, such as ammonium, formate, and guanidinium, were chosen to represent Lys, Asp, Glu, and Arg residues, respectively, along with the zwitterionic ions found at the first and last residues of a protein sequence. Methanol was used for the OH part of Tyr, Thr, and Ser, while methanethiol was used to parametrize any sulfur-containing residues, such as Met and Cys.

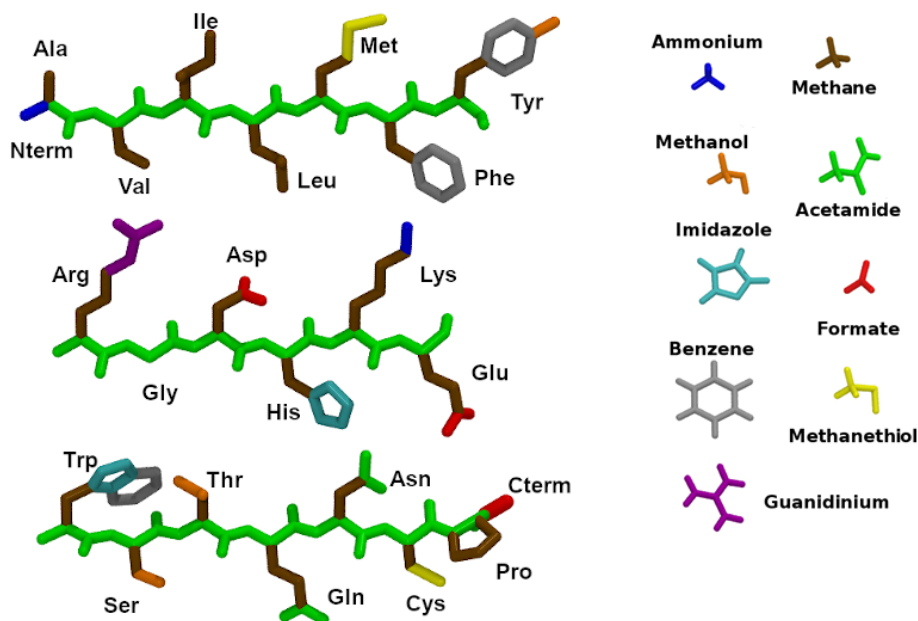


Figure 3: Left, atom-types reported for the protein force-field implemented in DockSurf software. Right, small molecules associated to the atom-types.

Association energies with gold surface were recorded with a minimal Au{111} surface as illustrated on the left part of figure 4. Each of the nine small molecules are then regularly move to the

surface according to its normal distance, also known as surface separation distance (SSD)⁴⁶. These computations were made in vacuum at the QM and MM levels.

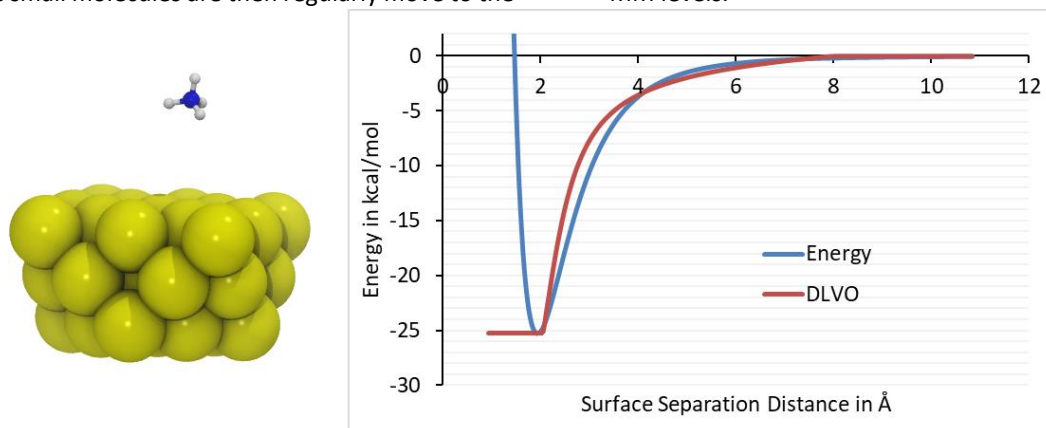


Figure 4: Left, illustration of the systems used for calculations with the minimal Au{111} surface and the set of molecules, here the ammonium, which are regularly approached to the surface. Right, association energy, in blue, computed for gold and ammonium according to the SSD distance and, in red, the DLVO potential of ammonium as described in the text.

With the potential energy in hands, as shown on the blue curve of the right part of figure 4, a simpler function was sought to decipher this potential with only the SSD as variable. To this extent, a specific potential, inspired from the work of Derjaguin, Landau, Verwey, and Overbeekhas (DLVO)⁴⁷ and their further improvement¹⁸, has been designed in this work. The goal of this potential is to provide an as simple as possible estimation of molecule/surface energy interaction as a function of the SSD value. To do this, the attractive part of the energy potential was fitted with a three parts curve according to:

$$\begin{aligned}
 & \text{if } SSD < SSD_{min} \rightarrow \text{Score}(SSD) = E_{min} \\
 & \text{if } thresh > SSD \geq SSD_{min} \rightarrow \\
 & \text{Score}(SSD) = \alpha/SSD + \beta/SSD^{12} + \gamma/SSD^6 + \delta \\
 & \text{if } SSD > thresh \text{ or } \text{Score}(SSD) > 0 \rightarrow \\
 & \text{Score}(SSD) = 0
 \end{aligned}$$

On these three equations, E_{min} and SSD_{min} were derived directly from the potential energy curves since these represent, respectively, the minimal energy with its corresponding SSD value. α , β , γ and δ are obtained with a polynomial fit. All these values, along with the correlation coefficient R^2 , are compiled in table S1 for all molecules and both set of theories. Thresh represents a cut-off value for which, beyond, no calculation is made. After several attempts, a value of 10 Å seems to represent a good

balance between accuracy and computational time. It is worth to note that the user can remove this thresh value in order to consider a no cut-off docking but it can be pointed that, in our investigations, no improvements were obtain confirming our previous works^{9,10,20,48-50} made on biomolecule/surface association for which no meaning interaction were recorded up to 10 Å above surface.

SSD corresponds to the Tz translation degree of freedom. By removing the repulsive part of the molecule surface energy association, the Tz exploration for any precession/nutation couple of values has no longer meaning. Indeed, for any rotational protein conformation, the lowest value of z will provide the value of 0 for the SSD. According to the fact that the repulsive part occurs for the closest atoms to the surface residues and occurs for SSD values between 0 to 3.5 Å (depending on the molecule, see table S1 for details). Considering only the attractive part by setting a ceiling value set to the minimal expected energy value, provides an astute assumption to avoid any exploration to this Tz variable. Consequently, the energies obtained are qualitative and not suitable for direct use in subsequent analyses. Nonetheless, it is worth noting that all molecular docking software provide qualitative energy computations and the aim of this study is to differentiate between multiple protein orientations.

Over the last years, our team has shown a keen interest to unveil the pivotal role water at the interface of surfaces such as gold, rutile, quartz and organic polymers^{9,21,46,48,49}. From these studies it can be drawn that water plays a role on adsorption only at the vicinity of the surface which can be qualitatively considered through a computation of generalized born solvation⁴⁶. Therefore, to compute quickly the solvent effect, the 9 molecules used as template for protein (cf. figure 3) were subjected to a 10 ns MD trajectory in a water box. Solvent contributions were then elucidated, for each of the 9 molecules, from the MMGBSA computational scheme^{51,52}. This technique has the advantage to consider the electrostatic component of solvent interaction (GB) along with the desolvation process as a proportion of its surface area (SA). On DockSurf software, the solvent contribution was just added on the final scoring equation to provide:

$$Score_{total} = \sum_{SSD=0}^{SSD < 10 \text{ \AA}} Score_{QM \text{ or } MM}^i(SSD) - \sum_{SSD=0}^{SSD < 2.8 \text{ \AA}} Solv^i(SSD)$$

Since de-solvation process acts at the vicinity of surface the SSD distance of 2.8 Å was stated to abate any interactions greater than this distance. In the range of 0 to 2.8 Å, the solvation score is not modulated by the distance but is constant according to the atomic type, defined by the 9 templates molecules. This choice was made in order to take into account the dynamical reorganization that occurs at the interface of gold surface. It is crucial to note that the solvent effect presented in this study is qualitative and primarily serves to regulate the results of the first scoring computation, whether from MM or QM, rather than providing a precise estimate of the adsorption free energy. Again, as with other molecular docking software, the scoring values produced by DockSurf, which have no unit, are intended to offer a relative/qualitative perspective rather than a quantitative one.

g) Mapping:

The most striking and specific result of the DockSurf software is to propose a mapping of the interaction between a protein and an inorganic surface according to the orientation of the biomolecule. An example of such results is shown on figure 5. To let the user choosing wisely the interaction structure(s) of its protein structure, the software produces 5 distinct mappings:

- The one made at MM level of theory (ΔH_{MM}).
- The one made at the QM level of theory (ΔH_{QM}).
- The one made of the solvation alone ($\Delta Solv$).
- The one adding the MM and solvation mappings (ΔG_{MM}).
- The one adding the QM and solvation mappings (ΔG_{QM}).

DockSurf software systematically generates the maps with the 5 above mentioned scorings and creates the protein complexes with the inorganic surface for the number of selected structures, as distinct files (in pdb format). The authors of this work strongly suggest that users systematically compare the ΔG_{QM} and ΔG_{MM} generated maps in order to confirm an orientation. If the user wants to look at only one score, the ΔG_{QM} map seems to be the most informative one since it takes into account the solvation along with polarization effect according to the QM computation. It is worth noting that despite their names, and like any molecular docking software, generated scorings are far from being comparable to real free energy computations.

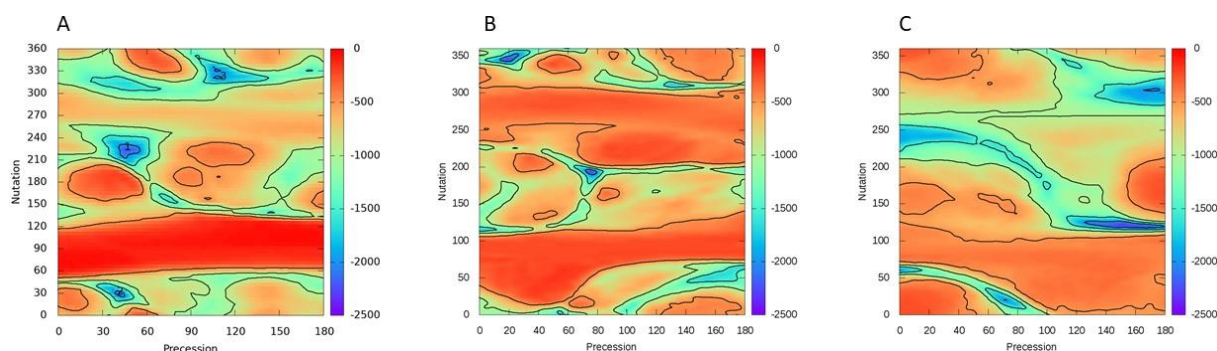


Figure 5: DockSurf results mapping obtained for, from left to right, serpin, human serum albumin and apolipoprotein. For convenience, only the ΔG_{QM} maps are shown.

h) Internet availability:

The development of a software program may hold limited value if its user base is confined to a restricted number of individuals (sometimes only by its creator). In order to enhance the reach of the DockSurf software, a concerted effort was made to integrate it into a web-based platform, thereby enabling its accessibility to a wider audience. Moreover, to circumvent the installation procedure, the software was implemented in the RPBS webserver to permit both online computation and analysis of outcomes in a user-friendly manner, thereby allowing DockSurf to be of value to a larger audience of researchers in the field, irrespective of their familiarity with molecular modeling. The web address to DockSurf is <https://bioserv.rpbs.univ-paris-diderot.fr/services/DockSurf/>

The RPBS webserver, where Docksurf is implemented, is directly linked to the protein databank so that only a 3 letters pdb code could be provided as input. Two type of outputs are generated. First, plots images are generated for the 5 different energy maps through Gnuplot and directly displayed on the webpage. Then, the asked number of the best protein structures associated to the surface are proposed, for each energy score, and can be downloaded. Finally, these structures can be directly visualized onto the web page through either the PV⁵³ or NGL⁵⁴ viewers. Figure 6 illustrates a typical output of DockSurf onto RPBS. DockSurf calculations are fast, typical calculation time for a protein of 200 amino acids is on the order of only few minutes, depending on server load.

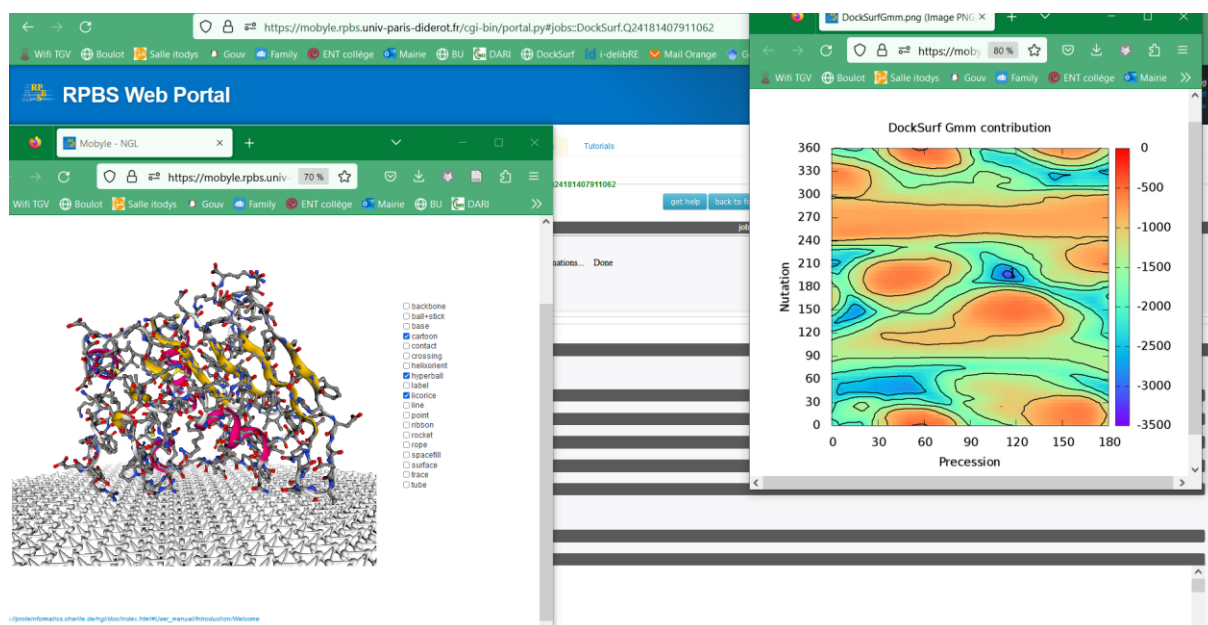


Figure 6: Screenshot illustrating the interface and use of the DockSurf webserver version.

Results and validations:

Classically, a molecular docking software is validated through the reproduction of experimental

structures such as protein/ligand complexes available on the protein databank website. However, there is no such experimental data available for protein adsorbed onto inorganic

surfaces such as gold. This lack of data prevents us a classical validation through a sample of relevant structural data. Therefore, various MD simulations was produced at the gold interface to confront and validate the molecular docking results of DockSurf.

To this extent, three different proteins, namely serpin, human serum albumin and apolipoprotein, were selected for their known ability to adsorb onto gold surfaces⁵⁵. The selection was based on the fact that these proteins have been structurally elucidated and exhibit versatile electrostatic potentials (as depicted in figure S1). Thus, their structural adsorption cannot be solely inferred from their global dipolar moment. Additionally, these proteins have various sizes, folding patterns, and secondary structural elements (see figure S1). Furthermore, these proteins are widely distributed in the human body, and their adsorption onto gold surfaces and nanoparticles is generally viewed as a barrier to the development of nanomaterials⁵⁵. Therefore, studying their adsorption properties is biologically significant.

It is of utmost importance to bear in mind that MD simulations neither computes energy and

Table 1: Serpin protein DockSurf results for the three first favourable association. Precession and nutation angles are in degrees while scorings values have no unit. ΔG_{MMGBSA} are in kcal/mol.

	Precession	Nutation	ΔG_{QM}	ΔG_{MM}	ΔG_{MMGBSA}
Pose 1	45	225	-2281.3	-4246.8	-534.1 \pm 7.2
Pose 2	40	30	-2135.8	-4085.8	-519.8 \pm 9.8
Pose 3	110	320	-2027.1	-3723.1	-493.3 \pm 8.4

Molecular dynamics were performed for 50 ns for the three distinct poses, in association with the gold surface embedded in water box. No restraint was imposed during the calculations so that the association was solely driven by the force-field. Figure S2 represents the evolution of the root mean square deviation (RMSD) of backbone atoms along the simulation time for each poses. Interestingly, the RMSD curves quickly reached a plateau and remained below 2 Å throughout the MD trajectory,

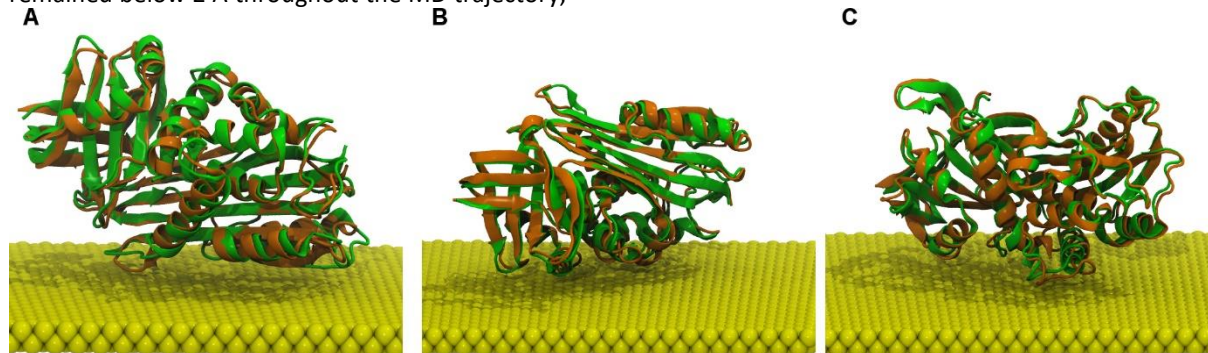


Figure 7: Serpin molecular dynamics simulations evolution from the DockSurf poses (green) and after 50 ns of MD simulations (orange). A, B and C stands for, respectively, poses 1, 2 and 3.

explore the conformational space as DockSurf software. As a result, any agreement between the results obtained using both methods provides compelling evidence of the validity and usefulness of the DockSurf software.

i) Serpin

Serpin stands for serine protease inhibitor. This protein controls an array of biological processes⁵⁶, such as coagulation and inflammation, so that its interaction toward a gold surface may modulates the biocompatibility of a biomaterial⁵⁷. The human serpin structure⁵⁸ (pdb code 1AS4) was studied with DockSurf software. Whole computations were made in 5 minutes onto a classical laptop and provides the map displayed on figure 5A. From this map, three relevant distinct conformations were identified and their precession and nutation angles along with their DockSurf scores are presented in table1. Interestingly, ΔG_{QM} and ΔG_{MM} present the same ranking for the three poses, indicating a similar behavior.

indicating the high stability of Serpin/gold complexes. This finding proves that our software was able to accurately identify relevant Serpin structures adsorbed onto the gold surface. Additionally, as shown in figure 6, despite the absence of restraints, all three Serpin docking poses remained structurally unchanged in the MD representative structures, confirming the stability of the complexes.

To distinguish between the three binding positions identified by the DockSurf software, free energies of binding were calculated using MMGBSA computations, and the results are summarized in Table 1. Although this method provides a rough estimate of the binding free energies, it is useful for understanding trends and observed affinities and has been successfully employed for biomolecules adsorbed to surface^{9,50}. The data in Table 1 indicate that all free energies are negative, as expected, suggesting a favorable interaction of Serpin with the gold surface for the three distinct binding positions. However, the free energies differ even after considering their standard deviations and follow the same ranking order as the DockSurf software. Therefore, more than validating the three binding positions, it can be concluded that DockSurf is capable of efficiently ranking the adsorbed conformations.

j) Human serum albumin and Apolipoprotein

Another strategy was employed to validate the DockSurf software for human serum albumin (HSA) and apolipoprotein. At first step, a mapping was generated for both proteins with the pdb codes 1N5U and 1LE2 for, respectively, the experimental structures of HSA⁵⁹ and apolipoprotein⁶⁰. According to the fact that the force-field and quantum-chemistry mapping was roughly identical, this last

map was used as reference and identify two favorable positions for HSA and three for apolipoprotein which can be visualized on the left panel of figure 7. These results are compiled in table 2. As remark, one interesting observation from this table is that the best docking poses get very similar score for either HSA or apolipoprotein (-2333.3 and -2336.9 respectively). Comparison of scoring between proteins systems should be made cautiously but can nevertheless being related with the fact that, in the paper of Garcia-Alvarez and collaborators⁵⁵, HSA and apolipoprotein are always encountered in the top 5 of the 20 most abundant proteins for their 12 mice *in-vivo* samples.

In order to assess the relevance of the docking poses obtained by the DockSurf software, it was decided to start similar MD simulations but with starting structures away from these mimimas. If the MD trajectories led to structures similar to those identified by DockSurf, this would validate the computed conformational maps. These starting positions are displayed on the right part of figure 8 and their Euler angles are reported in table 2. After 100 and 200 ns of MD simulations for, respectively, HSA and apolipoprotein the nutation and precession angles were computed for the last 10 ns of simulations. These last values along with their standard deviations are reported in table 2.

Table 2: Results of DockSurf for HSA and Apolipoprotein. ΔG_{qm} is the DockSurf scoring values. 'Best', 'Start' and 'MD' represent, respectively, the most favourable interaction computed with DockSurf, the selected starting position of both protein and their average positions issued from the last 10 ns of molecular dynamics trajectories.

System	HAS			Apolipoprotein		
	precession	nutation	ΔG_{qm}	precession	nutation	ΔG_{qm}
Best	20	345	-2333.3	150	130	-2336.9
Start	45	315	-650.45	80	110	-646.9
MD	22 ± 7.7	338 ± 4.8		144 ± 4.5	126 ± 2.0	

The most striking results from these analyses is the very good convergence of the results obtained from MD trajectories and the highlighted best docking poses from DockSurf. This strongly support these favorable positions of protein onto the gold surfaces. Besides, a supplemental analysis was performed to report these dihedral angles along the MD trajectories. These values are plotted onto the mappings elucidated by DockSurf and displayed on the middle panel of figure 7. It is remarkable to observe

that, for both systems, the pathways of molecular dynamics follow the mountains and valleys of our software conformational maps.

The consistency of the results obtained from both methods for Serpin, HSA, and apolipoprotein indicates that DockSurf is a useful tool for quickly identifying favorable binding positions on solid surfaces, especially given the time and expertise required for MD simulations.

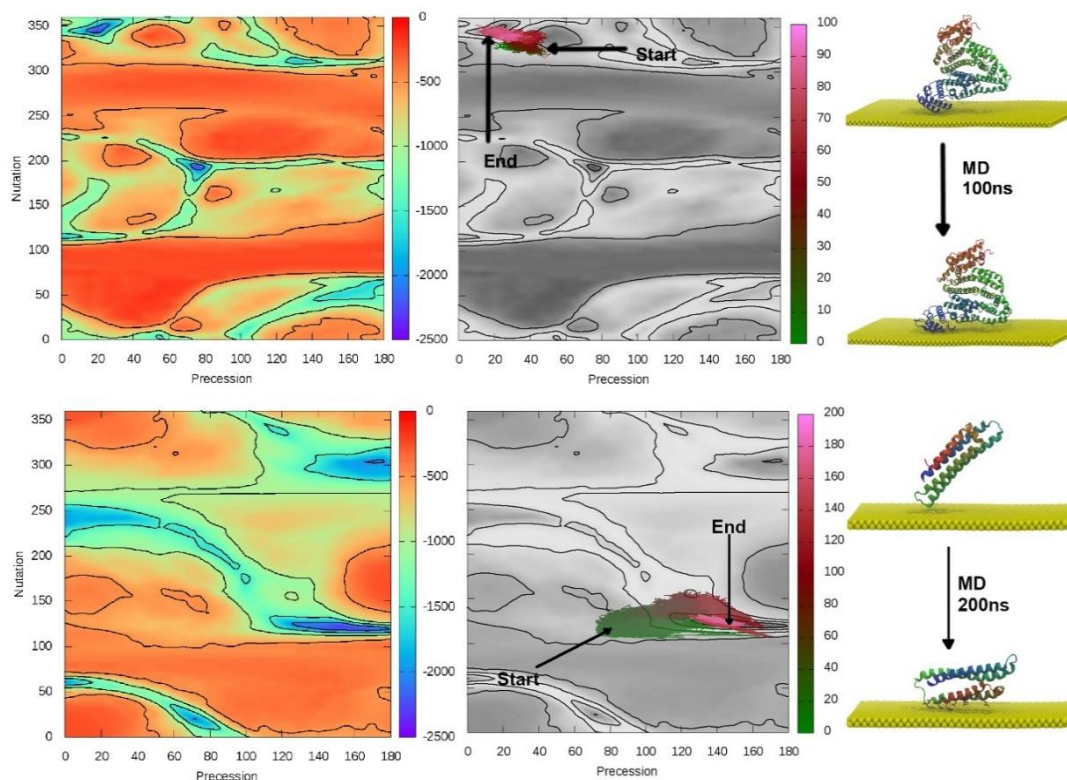


Figure 8: Results from molecular dynamics simulations of HSA (top) and apolipoprotein (bottom). From left to right: DockSurf results mapping indicating the best positions for both protein systems; Starting and final positions of the molecular dynamics simulations shown with arrows for both systems in the middle; illustrations, on the right panel, of these MD evolutions. For this last representation, water molecules and ions are removed for the sake of clarity.

Conclusions and prospects:

In this study we develop a software to quickly predict the orientation and interaction of a protein onto a planar inorganic surface. In that intention, a specific all-atom force-field for protein was parameterized with QM computation to encompass as much as possible physical effects at the interface. An original exploration strategy authorizes a more exhaustive computations of protein/surface adsorption leading the identification of several favorable binding poses. As far as we know, there is no experimental structure at the atomic scale of protein immobilized onto an inorganic surface so that the validation of DockSurf was made with intensive MD calculations. Convergence of results was astounding and strongly validate the approach of DockSurf. Besides, this software is freely accessible on a website and can be launch easily from an internet browser. This website is directly linked to the protein databank and propose visualization tools for the resulting conformational maps and protein coordinates, so that DockSurf could be used without any computational knowledge and remains accessible for a broad audience.

DockSurf is limited to Au{111} surfaces and proteins. However, extension to other biomolecules, such as nucleic acids, and surfaces will be further realized. In fact, the inherent parameters for each type of surface are cleverly placed at the beginning of the program, allowing the possibility of adding new parameters without having to read and understand the program. This will allow to easily enrich the number of mineral or organic surfaces.

Acknowledgements:

ANR (Agence Nationale de la Recherche) and CGI (Commissariat à l'Investissement d'Avenir) are gratefully acknowledged for their financial support of this work through Labex SEAM (Science and Engineering for Advanced Materials and devices) ANR 11 LABX 086, ANR 11 IDEX 05 02. This work benefited from the access to the supercomputing facilities of the GENCI (Grand Equipement National pour le Calcul Informatique).

References:

- (1) Ozboyaci, M.; Koh, D. B.; Corni, S.; Wade, R. C. Modeling and Simulation of Protein–Surface Interactions: Achievements and Challenges. *Quart. Rev. Biophys.* **2016**, *49*, e4. <https://doi.org/10.1017/S0033583515000256>.

- (2) Mann, S. Molecular Recognition in Biomaterialization. *Nature* **1988**, *332*, 119–124.
- (3) Silva-Bermudez, P.; Rodil, S. E. An Overview of Protein Adsorption on Metal Oxide Coatings for Biomedical Implants. *Surface and Coatings Technology* **2013**, *233*, 147–158. <https://doi.org/10.1016/j.surfcoat.2013.04.028>.
- (4) Liong, M.; Lu, J.; Kovochich, M.; Xia, T.; Ruehm, S. G.; Nel, A. E.; Tamanoi, F.; Zink, J. I. Multifunctional Inorganic Nanoparticles for Imaging, Targeting, and Drug Delivery. *ACS Nano* **2008**, *2* (5), 889–896. <https://doi.org/10.1021/nn800072t>.
- (5) Nel, A.; Xia, T. Toxic Potential of Materials at the Nanoscale. *Science* **2006**, *311*, 622–627.
- (6) Nguyen, T. T. K.; Nguyen, T. N.; Anquetin, G.; Reisberg, S.; Noël, V.; Mattana, G.; Touzeau, J.; Barbault, F.; Pham, M. C.; Piro, B. Triggering the Electrolyte-Gated Organic Field-Effect Transistor Output Characteristics through Gate Functionalization Using Diazonium Chemistry: Application to Biodetection of 2,4-Dichlorophenoxyacetic Acid. *Biosensors and Bioelectronics* **2018**, *113*, 32–38. <https://doi.org/10.1016/j.bios.2018.04.051>.
- (7) Dalsin, J. L.; Messersmith, P. B. Bioinspired Antifouling Polymers. *Materials Today* **2005**, *8* (9), 38–46. [https://doi.org/10.1016/S1369-7021\(05\)71079-8](https://doi.org/10.1016/S1369-7021(05)71079-8).
- (8) Statz, A. R.; Meagher, R. J.; Barron, A. E.; Messersmith, P. B. New Peptidomimetic Polymers for Antifouling Surfaces. *J. Am. Chem. Soc.* **2005**, *127* (22), 7972–7973. <https://doi.org/10.1021/ja0522534>.
- (9) Mazouz, Z.; Mokni, M.; Fourati, N.; Zerrouki, C.; Barbault, F.; Seydou, M.; Kalfat, R.; Yaakoubi, N.; Omezzine, A.; Bouslema, A.; Othmane, A. Computational Approach and Electrochemical Measurements for Protein Detection with MIP-Based Sensor. *Biosensors and Bioelectronics* **2020**, *151*, 111978. <https://doi.org/10.1016/j.bios.2019.111978>.
- (10) Ktari, N.; Fourati, N.; Zerrouki, C.; Ruan, M.; Seydou, M.; Barbault, F.; Nal, F.; Yaakoubi, N.; Chehimi, M. M.; Kalfat, R. Design of a Polypyrrole MIP-SAW Sensor for Selective Detection of Fluoroquinolone in Aqueous Media. Correlation between Experimental Results and DFT Calculations. *RSC Adv.* **2015**, *5* (108), 88666–88674. <https://doi.org/10.1039/C5RA16237H>.
- (11) Skelton, A. A.; Liang, T.; Walsh, T. R. Interplay of Sequence, Conformation, and Binding at the Peptide–Titania Interface as Mediated by Water. *ACS Appl. Mater. Interfaces* **2009**, *1* (7), 1482–1491. <https://doi.org/10.1021/am9001666>.
- (12) Costa, D.; Garrain, P.-A.; Baaden, M. Understanding Small Biomolecule–Biomaterial Interactions: A Review of Fundamental Theoretical and Experimental Approaches for Biomolecule Interactions with Inorganic Surfaces. *J. Biomed. Mater. Res.* **2013**, *101A* (4), 1210–1222. <https://doi.org/10.1002/jbm.a.34416>.
- (13) Heinz, H.; Lin, T.-J.; Kishore Mishra, R.; Emami, F. S. Thermodynamically Consistent Force Fields for the Assembly of Inorganic, Organic, and Biological Nanostructures: The INTERFACE Force Field. *Langmuir* **2013**, *29* (6), 1754–1765. <https://doi.org/10.1021/la3038846>.
- (14) Heinz, H.; Vaia, R. A.; Farmer, B. L.; Naik, R. R. Accurate Simulation of Surfaces and Interfaces of Face-Centered Cubic Metals Using 12–6 and 9–6 Lennard-Jones Potentials. *J. Phys. Chem. C* **2008**, *112* (44), 17281–17290. <https://doi.org/10.1021/jp801931d>.
- (15) Hoefling, M.; Iori, F.; Corni, S.; Gottschalk, K.-E. Interaction of Amino Acids with the Au(111) Surface: Adsorption Free Energies from Molecular Dynamics Simulations. *Langmuir* **2010**, *26* (11), 8347–8351. <https://doi.org/10.1021/la904765u>.
- (16) Collier, G.; Vellore, N. A.; Yancey, J. A.; Stuart, S. J.; Latour, R. A. Comparison Between Empirical Protein Force Fields for the Simulation of the Adsorption Behavior of Structured LK Peptides on Functionalized Surfaces. *Biointerphases* **2012**, *7* (1), 24. <https://doi.org/10.1007/s13758-012-0024-z>.
- (17) Snyder, J. A.; Abramyan, T.; Yancey, J. A.; Thyparambil, A. A.; Wei, Y.; Stuart, S. J.; Latour, R. A. Development of a Tuned Interfacial Force Field Parameter Set for the Simulation of Protein Adsorption to Silica Glass. *Biointerphases* **2012**, *7* (1), 56. <https://doi.org/10.1007/s13758-012-0056-4>.
- (18) Vellore, N. A.; Yancey, J. A.; Collier, G.; Latour, R. A.; Stuart, S. J. Assessment of the Transferability of a Protein Force Field for the Simulation of Peptide–Surface Interactions. *Langmuir* **2010**, *26* (10), 7396–7404. <https://doi.org/10.1021/la904415d>.
- (19) Steinmann, S. N.; Fleurat-Lessard, P.; Götz, A. W.; Michel, C.; Ferreira de Moraes, R.; Sautet, P. Molecular Mechanics Models for the Image Charge, a Comment on “Including Image Charge Effects in the Molecular Dynamics Simulations of Molecules on Metal Surfaces.” *J. Comput. Chem.* **2017**, *38* (24), 2127–2129. <https://doi.org/10.1002/jcc.24861>.
- (20) Hitaishi, V.; Clement, R.; Bourassin, N.; Baaden, M.; de Poulpique, A.; Sacquin-Mora, S.; Ciaccafava, A.; Lojou, E. Controlling Redox Enzyme Orientation at Planar Electrodes. *Catalysts* **2018**, *8* (5), 192. <https://doi.org/10.3390/catal8050192>.
- (21) Bourassin, N.; Barbault, F.; Baaden, M.; Sacquin-Mora, S. Between Two Walls: Modeling the Adsorption Behavior of β -Glucosidase A on Bare and SAM-Functionalized Gold Surfaces. *Langmuir* **2022**, *38* (4), 1313–1323. <https://doi.org/10.1021/acs.langmuir.1c01774>.
- (22) Xie, Y.; Liu, M.; Zhou, J. Molecular Dynamics Simulations of Peptide Adsorption on Self-Assembled Monolayers. *Applied Surface Science* **2012**, *258* (20), 8153–8159. <https://doi.org/10.1016/j.apsusc.2012.05.013>.
- (23) Freeman, C. L.; Harding, J. H.; Quigley, D.; Rodger, P. M. Simulations of Ovocleidin-17 Binding to Calcite Surfaces and Its Implications for Eggshell Formation. *J. Phys. Chem. C* **2011**, *115* (16), 8175–8183. <https://doi.org/10.1021/jp200145m>.
- (24) Kubiak-Ossowska, K.; Mulheran, P. A.; Nowak, W. Fibronectin Module FN^{III} 9 Adsorption at Contrasting Solid Model Surfaces Studied by Atomistic Molecular Dynamics. *J. Phys. Chem. B* **2014**, *118* (33), 9900–9908. <https://doi.org/10.1021/jp5020077>.
- (25) Leach, A. R.; AR, L. *Molecular Modelling: Principles and Applications*; Pearson Education, 2001.
- (26) Barbault, F.; Zhang, L.; Zhang, L.; Fan, B. T. Parametrization of a Specific Free Energy Function for Automated Docking against RNA Targets Using Neural Networks. *Chemometrics and Intelligent Laboratory Systems* **2006**, *82* (1–2), 269–275. <https://doi.org/10.1016/j.chemolab.2005.05.014>.
- (27) Barbault, F.; Ren, B.; Rebehmed, J.; Teixeira, C.; Luo, Y.; Smila-Castro, O.; Maurel, F.; Fan, B.; Zhang, L.; Zhang, L. Flexible Computational Docking Studies of New Aminoglycosides Targeting RNA 16S Bacterial Ribosome Site. *European Journal of Medicinal Chemistry* **2008**, *43* (8), 1648–1656. <https://doi.org/10.1016/j.ejmech.2007.10.022>.
- (28) Li, A.; Maurel, F.; Barbault, F.; Delamar, M.; Wang, B.; Zhou, X.; Wang, P. Molecular Modeling Study of Binding Site Selectivity of TQMP to G-Quadruplex DNA. *European Journal of Medicinal Chemistry* **2010**, *45* (3), 983–991. <https://doi.org/10.1016/j.ejmech.2009.11.040>.
- (29) Martins, M.; Pluvinage, B.; de la Sierra-Gallay, I. L.; Barbault, F.; Dairou, J.; Dupret, J.-M.; Rodrigues-Lima, F.

- Functional and Structural Characterization of the Arylamine N-Acetyltransferase from the Opportunistic Pathogen *Nocardia Farcinica*. *Journal of Molecular Biology* **2008**, *383* (3), 549–560. <https://doi.org/10.1016/j.jmb.2008.08.035>.
- (30) Han, T. H. L.; Camadro, J.-M.; Barbault, F.; Santos, R.; El Hage Chahine, J.-M.; Ha-Duong, N.-T. In Vitro Interaction between Yeast Frataxin and Superoxide Dismutases: Influence of Mitochondrial Metals. *Biochimica et Biophysica Acta (BBA) - General Subjects* **2019**, *1863* (5), 883–892. <https://doi.org/10.1016/j.bbagen.2019.02.011>.
- (31) Frisch, M. J.; Trucks, G. W.; Schlegel, H. B.; Scuseria, G. E.; Robb, M. A.; Cheeseman, J. R.; Scalmani, G.; Barone, V.; Petersson, G. A.; Nakatsuji, H.; Li, X.; Caricato, M.; Marenich, A. V.; Bloino, J.; Janesko, B. G.; Gomperts, R.; Mennucci, B.; Hratchian, H. P.; Ortiz, J. V.; Izmaylov, A. F.; Sonnenberg, J. L.; Williams, Ding, F.; Lipparini, F.; Egidi, F.; Goings, J.; Peng, B.; Petrone, A.; Henderson, T.; Ranasinghe, D.; Zakrzewski, V. G.; Gao, J.; Rega, N.; Zheng, G.; Liang, W.; Hada, M.; Ehara, M.; Toyota, K.; Fukuda, R.; Hasegawa, J.; Ishida, M.; Nakajima, T.; Honda, Y.; Kitao, O.; Nakai, H.; Vreven, T.; Throssell, K.; Montgomery Jr., J. A.; Peralta, J. E.; Ogliaro, F.; Bearpark, M. J.; Heyd, J. J.; Brothers, E. N.; Kudin, K. N.; Staroverov, V. N.; Keith, T. A.; Kobayashi, R.; Normand, J.; Raghavachari, K.; Rendell, A. P.; Burant, J. C.; Iyengar, S. S.; Tomasi, J.; Cossi, M.; Millam, J. M.; Klene, M.; Adamo, C.; Cammi, R.; Ochterski, J. W.; Martin, R. L.; Morokuma, K.; Farkas, O.; Foresman, J. B.; Fox, D. J. *Gaussian 16 Rev. C.01*, 2016.
- (32) Wang, J.; Wolf, R. M.; Caldwell, J. W.; Kollman, P. A.; Case, D. A. Development and Testing of a General Amber Force Field. *J. Comput. Chem.* **2004**, *25* (9), 1157–1174. <https://doi.org/10.1002/jcc.20035>.
- (33) Case, D. A.; Belfon, K.; Ben-Shalom, I. Y.; Brozell, S. R.; Cerutti, D. S.; Cheatham III, T. E.; Cruzeiro, V. W. D.; Darden, T. A.; Duke, R. E.; Giambasu, G.; Gilson, M. K.; Gohlke, H.; Goetz, A. W.; Harris, R.; Izadi, S.; Izmailov, S. A.; Kasavajhala, K.; Kovalenko, A.; Krasny, R.; Kurtzman, T.; Lee, T. S.; LeGrand, S.; Li, P.; Lin, C.; Liu, J.; Luchko, T.; Luo, R.; Man, V.; Merz, K. M.; Miao, Y.; Mikhailovskii, O.; Monard, G.; Nguyen, H.; Onufriev, A.; Pan, F.; Pantano, S.; Qi, R.; Roe, D. R.; Roitberg, A.; Sagui, C.; Schott-Verdugo, S.; Shen, J.; Simmerling, C. L.; Skrynnikov, N. R.; Smith, J.; Swails, J.; Walker, R. C.; Wang, J.; Wilson, L.; Wolf, R. M.; Wu, X.; Xiong, Y.; Xue, Y.; York, D. M.; Kollman, P. A. *Amber 20*, 2020.
- (34) Maier, J. A.; Martinez, C.; Kasavajhala, K.; Wickstrom, L.; Hauser, K. E.; Simmerling, C. Ff14SB: Improving the Accuracy of Protein Side Chain and Backbone Parameters from Ff99SB. *J. Chem. Theory Comput.* **2015**, *11* (8), 3696–3713. <https://doi.org/10.1021/acs.jctc.5b00255>.
- (35) Jorgensen, W. L.; Chandrasekhar, J.; Madura, J. D.; Impey, R. W.; Klein, M. L. Comparison of Simple Potential Functions for Simulating Liquid Water. *The Journal of Chemical Physics* **1983**, *79* (2), 926–935. <https://doi.org/10.1063/1.445869>.
- (36) Humphrey, W.; Dalke, A.; Schulten, K. VMD: Visual Molecular Dynamics. *Journal of Molecular Graphics* **1996**, *14* (1), 33–38. [https://doi.org/10.1016/0263-7855\(96\)00018-5](https://doi.org/10.1016/0263-7855(96)00018-5).
- (37) Roe, D. R.; Cheatham, T. E. PTRAJ and CPPTRAJ: Software for Processing and Analysis of Molecular Dynamics Trajectory Data. *J. Chem. Theory Comput.* **2013**, *9* (7), 3084–3095. <https://doi.org/10.1021/ct400341p>.
- (38) Kollman, P. A.; Massova, I.; Reyes, C.; Kuhn, B.; Huo, S.; Chong, L.; Lee, M.; Lee, T.; Duan, Y.; Wang, W.; Donini, O.; Cieplak, P.; Srinivasan, J.; Case, D. A.; Cheatham, T. E. Calculating Structures and Free Energies of Complex Molecules: Combining Molecular Mechanics and Continuum Models. *Acc. Chem. Res.* **2000**, *33* (12), 889–897. <https://doi.org/10.1021/ar000033j>.
- (39) Berman, H. M.; Westbrook, J.; Feng, Z.; Gilliland, G.; Bhat, T. N.; Weissig, H.; Shindyalov, I. N.; Bourne, P. E. The Protein Data Bank. *Nucleic Acids Res* **2000**, *28* (1), 235–242. <https://doi.org/10.1093/nar/28.1.235>.
- (40) Williams, T.; Kelley, C. *Gnuplot: an interactive plotting program*. <http://gnuplot.info/> (accessed 2022-07-25).
- (41) Alland, C.; Moreews, F.; Boens, D.; Carpentier, M.; Chiusa, S.; Lonquety, M.; Renault, N.; Wong, Y.; Cantalloube, H.; Chomilier, J.; Hochez, J.; Pothier, J.; Villoutreix, B. O.; Zagury, J.-F.; Tuffery, P. RPBS: A Web Resource for Structural Bioinformatics. *Nucleic Acids Research* **2005**, *33* (Web Server), W44–W49. <https://doi.org/10.1093/nar/gki477>.
- (42) Néron, B.; Ménager, H.; Maufrais, C.; Joly, N.; Maupetit, J.; Letort, S.; Carrere, S.; Tuffery, P.; Letondal, C. Mobyle: A New Full Web Bioinformatics Framework. *Bioinformatics* **2009**, *25* (22), 3005–3011. <https://doi.org/10.1093/bioinformatics/btp493>.
- (43) Bonvin, A. M. Flexible Protein–Protein Docking. *Current Opinion in Structural Biology* **2006**, *16* (2), 194–200. <https://doi.org/10.1016/j.sbi.2006.02.002>.
- (44) Morris, G. M.; Huey, R.; Lindstrom, W.; Sanner, M. F.; Belew, R. K.; Goodsell, D. S.; Olson, A. J. AutoDock4 and AutoDockTools4: Automated Docking with Selective Receptor Flexibility. *J. Comput. Chem.* **2009**, *30* (16), 2785–2791. <https://doi.org/10.1002/jcc.21256>.
- (45) Trott, O.; Olson, A. J. AutoDock Vina: Improving the Speed and Accuracy of Docking with a New Scoring Function, Efficient Optimization, and Multithreading. *J. Comput. Chem.* **2009**, NA-NA. <https://doi.org/10.1002/jcc.21334>.
- (46) Touzeau, J.; Seydou, M.; Maurel, F.; Tallet, L.; Mutschler, A.; Lavalle, P.; Barbault, F. Theoretical and Experimental Elucidation of the Adsorption Process of a Bioinspired Peptide on Mineral Surfaces. *Langmuir* **2021**, *37* (38), 11374–11385. <https://doi.org/10.1021/acs.langmuir.1c01994>.
- (47) Overbeek, J. T. G. Recent Developments in the Understanding of Colloid Stability. *Journal of Colloid and Interface Science* **1977**, *58* (2), 15.
- (48) Ruan, M.; Seydou, M.; Noel, V.; Piro, B.; Maurel, F.; Barbault, F. Molecular Dynamics Simulation of a RNA Aptasensor. *J. Phys. Chem. B* **2017**, *121* (16), 4071–4080. <https://doi.org/10.1021/acs.jpcc.6b12544>.
- (49) Araujo-Rocha, M.; Piro, B.; Noël, V.; Barbault, F. Computational Studies of a DNA-Based Aptasensor: Toward Theory-Driven Transduction Improvement. *J. Phys. Chem. B* **2021**, *125* (33), 9499–9506. <https://doi.org/10.1021/acs.jpcc.1c05341>.
- (50) Touzeau, J.; Barbault, F.; Maurel, F.; Seydou, M. Insights on Porphyrin-Functionalized Graphene: Theoretical Study of Substituent and Metal-Center Effects on Adsorption. *Chemical Physics Letters* **2018**, *713*, 172–179. <https://doi.org/10.1016/j.cpl.2018.10.046>.
- (51) Hou, T.; Wang, J.; Li, Y.; Wang, W. Assessing the Performance of the MM/PBSA and MM/GBSA Methods. 1. The Accuracy of Binding Free Energy Calculations Based on Molecular Dynamics Simulations. *J. Chem. Inf. Model.* **2011**, *51* (1), 69–82. <https://doi.org/10.1021/ci100275a>.
- (52) Wang, E.; Sun, H.; Wang, J.; Wang, Z.; Liu, H.; Zhang, J. Z. H.; Hou, T. End-Point Binding Free Energy Calculation with MM/PBSA and MM/GBSA: Strategies and Applications in Drug Design. *Chem. Rev.* **2019**, *119* (16), 9478–9508. <https://doi.org/10.1021/acs.chemrev.9b00055>.

- (53) *PV - JavaScript Protein Viewer*.
<http://biasmv.github.io/pv/index.html> (accessed 2023-04-04).
- (54) Rose, A. S.; Bradley, A. R.; Valasatava, Y.; Duarte, J. M.; Prlić, A.; Rose, P. W. NGL Viewer: Web-Based Molecular Graphics for Large Complexes. *Bioinformatics* **2018**, *34* (21), 3755–3758.
<https://doi.org/10.1093/bioinformatics/bty419>.
- (55) García-Álvarez, R.; Hadjidemetriou, M.; Sánchez-Iglesias, A.; Liz-Marzán, L. M.; Kostarelos, K. *In Vivo* Formation of Protein Corona on Gold Nanoparticles. The Effect of Their Size and Shape. *Nanoscale* **2018**, *10* (3), 1256–1264. <https://doi.org/10.1039/C7NR08322J>.
- (56) Stein, P. E.; Carrell, R. W. What Do Dysfunctional Serpins Tell Us about Molecular Mobility and Disease? *Nat Struct Mol Biol* **1995**, *2* (2), 96–113.
<https://doi.org/10.1038/nsb0295-96>.
- (57) Bolaños, K.; Kogan, M. J.; Araya, E. Capping Gold Nanoparticles with Albumin to Improve Their Biomedical Properties. *IJN* **2019**, *Volume 14*, 6387–6406.
<https://doi.org/10.2147/IJN.S210992>.
- (58) Lukacs, C. M.; Rubin, H.; Christianson, D. W. Engineering an Anion-Binding Cavity in Antichymotrypsin Modulates the “Spring-Loaded” Serpin–Protease Interaction. *Biochemistry* **1998**, *37* (10), 3297–3304.
<https://doi.org/10.1021/bi972359e>.
- (59) Wardell, M.; Wang, Z.; Ho, J. X.; Robert, J.; Ruker, F.; Ruble, J.; Carter, D. C. The Atomic Structure of Human Methemalbumin at 1.9 Å. *Biochemical and Biophysical Research Communications* **2002**, *291* (4), 813–819.
<https://doi.org/10.1006/bbrc.2002.6540>.
- (60) Wilson, C.; Mau, T.; Weisgraber, K. H.; Wardell, M. R.; Mahley, R. W.; Agard, D. A. Salt Bridge Relay Triggers Defective LDL Receptor Binding by a Mutant Apolipoprotein. *Structure* **1994**, *2* (8), 713–718.
[https://doi.org/10.1016/S0969-2126\(00\)00072-1](https://doi.org/10.1016/S0969-2126(00)00072-1).